

Quantum Computing with Cluster States

Gelo Noel M. Tabia *

Perimeter Institute for Theoretical Physics,
31 Caroline Street North, Waterloo, Ontario, Canada N2L 2Y5
Institute for Quantum Computing and University of Waterloo,
200 University Avenue West, Waterloo, Ontario, Canada N2L 3G1

15 April 2011

Summary

In cluster state quantum computing, we start with a given fixed entangled state of many qubits called a cluster state and perform a quantum computation by applying a time-ordered sequence of single-qubit measurements to designated qubits in designated bases. The choice of basis for later measurements generally depend on the outcome of earlier measurements and the final result of the computation is determined from the classical information involving all measurement outcomes. This is in contrast to the more conventional network gate model of quantum computing, in which computational steps are unitary transformations. We describe how the underlying computational model of cluster state is different from the network model, in particular emphasizing how cluster state computers have no true notion of input and output registers. Nonetheless, we show that the two quantum computing models are equivalent by demonstrating how cluster states can be used to simulate quantum circuits efficiently. At the end, we include a short account on how to produce optical cluster states.

*Email: gtabia@perimeterinstitute.ca (UW ID: 20294659)

Table of Contents

1	Introduction	1
2	What are cluster states?	1
3	Universality of cluster-state quantum computing	3
3.1	Simulating quantum circuits	3
3.2	Random measurement outcomes	8
3.3	Sequence of simulated quantum gates	8
3.4	Efficiency of simulating quantum gates	9
4	Computational model for the cluster-state quantum computer	11
4.1	Non-network character of cluster state computing	11
4.2	A cluster-state computational model	12
5	Optical implementation of cluster states	13
5.1	Cluster states and the Knill-Laflamme-Milburn (KLM) proposal	13
5.2	Practical optical cluster state	15
6	Concluding remarks	16

1 Introduction

A quantum computer promises efficient information processing of some computational tasks that are believed to be intractable with classical computers. Standard quantum computing models are based on the paradigm of quantum logic networks, where a sequence of unitary quantum gates form the computational circuit. The one-way quantum computer proposed by Raussendorf and Briegel [1] provides an alternative model for scalable quantum computing in which a specific form of a highly entangled multi-particle state, called a *cluster state*, plays the pivotal role of being a universal resource for quantum computation. To perform a quantum algorithm with a cluster state, individual qubits are measured in a temporal sequence of adaptive single-qubit measurements with classical feed-forward processing of outcomes. The classical readout for such a quantum computation essentially involves all measurement outcomes of the cluster qubits.

In this project, we provide some basic details about cluster state quantum computing. Firstly, we define what cluster states are and how they can be realized from a Hamiltonian. Secondly, we show that cluster states are resources for universal quantum computing by showing how they can be imprinted with a simulated quantum circuit using single qubit rotations and CNOT gates. After that, we show how the random outcomes of individual qubit measurements do not affect the ability of a cluster state to perform an algorithm efficiently and how any necessary correction of Pauli errors due to these random outcomes can be delayed until the end of the computation. We follow that with a discussion on the non-network aspects of cluster state computing and provide a different computational model for cluster states that involves the temporal ordering of single-qubit measurements and an information flow vector that tracks the evolution of logical qubits. Lastly, we describe how cluster states can be created experimentally using polarization of photons and standard linear optical devices.

2 What are cluster states?

A cluster state is a set of qubits arranged in a d -dimensional lattice at sites $a \in \mathbb{Z}^d$ that couple via some short-range interaction with Hamiltonian

$$H_{\text{int}} = \hbar g(t) \sum_{a,a'} f(a-a') \frac{1+Z_a}{2} \frac{1-Z_{a'}}{2} \quad (1)$$

where

$$Z_a|0\rangle_a = |0\rangle_a, \quad Z_a|1\rangle_a = -|1\rangle_a \quad (2)$$

defines the Pauli-Z operator. With respect to the entanglement properties of cluster states relevant to quantum computing, this Hamiltonian is equivalent to the quantum Ising model at low temperatures:

$$H_{\text{Ising}} = - \sum_{a,a'} \hbar g(t) f(a-a') Z_a Z_{a'}. \quad (3)$$

They are equivalent in the sense that the states generated by H_{int} and H_{Ising} from a given initial state are identical up to local unitary transformations applied to individual qubits.

In principle, only next-neighbor interactions are needed to generate a cluster state from eq. (1). In such a case, H_{int} realizes simultaneous conditional phase gates between qubits at adjacent sites a and a' . For example, if we have a linear chain of N qubits then we can produce a cluster state using H_{int} with $f(a-a') = \delta_{a,a'+1}$.

Suppose we have a linear chain of qubits all initially in the state

$$|+\rangle_a = \frac{|0\rangle_a + |1\rangle_a}{\sqrt{2}} \quad (4)$$

then for $\varphi = \int g(t) dt$, the unitary evolution

$$U(\varphi) = \exp\left(-i\varphi \sum_a \frac{1+Z_a}{2} \frac{1-Z_{a+1}}{2}\right) \quad (5)$$

yields a disentangled chain for $\varphi = 2(k-1)\pi$ and a ‘maximally entangled’ one for $\varphi = (2k-1)\pi$, where $k \in \mathbb{Z}^+$.

For $\varphi = \pi$, the cluster state for a linear chain C_N of N qubits can be written in compact notation as

$$|\phi\rangle_{C_N} = \frac{1}{\sqrt{2^N}} \bigotimes_{a=1}^N (|0\rangle_a Z_{a+1} + |1\rangle_a) \quad (6)$$

where $Z_{N+1} = \mathbf{1}$ by definition, since it is impossible to entangle with an empty site.

Examples of the smallest linear cluster states are as follows:

$$|\phi\rangle_{C_2} = \frac{1}{\sqrt{2}} (|0\rangle|+\rangle + |1\rangle|-\rangle), \quad (7)$$

$$|\phi\rangle_{C_3} = \frac{1}{\sqrt{2}} (|+\rangle|0\rangle|+\rangle + |-\rangle|1\rangle|-\rangle), \quad (8)$$

$$|\phi\rangle_{C_4} = \frac{1}{2} (|+\rangle|0\rangle|+\rangle|0\rangle + |+\rangle|0\rangle|-\rangle|1\rangle + |-\rangle|1\rangle|-\rangle|0\rangle + |-\rangle|1\rangle|+\rangle|1\rangle), \quad (9)$$

which up to local unitary transformations on single qubits are equivalent to

$$|\phi\rangle_{C_2} \stackrel{l.u.}{=} \frac{1}{\sqrt{2}} (|0\rangle|0\rangle + |1\rangle|1\rangle), \quad (10)$$

$$|\phi\rangle_{C_3} \stackrel{l.u.}{=} \frac{1}{\sqrt{2}} (|0\rangle|0\rangle|0\rangle + |1\rangle|1\rangle|1\rangle), \quad (11)$$

$$|\phi\rangle_{C_4} \stackrel{l.u.}{=} \frac{1}{2} (|0\rangle|0\rangle|0\rangle|0\rangle + |0\rangle|0\rangle|1\rangle|1\rangle + |1\rangle|1\rangle|0\rangle|0\rangle - |1\rangle|1\rangle|1\rangle|1\rangle). \quad (12)$$

Observe that $|\phi\rangle_{C_2}$ is effectively a Bell state, $|\phi\rangle_{C_3}$ is effectively a 3-qubit GHZ state but $|\phi\rangle_{C_4}$ is not the same as the $|\text{GHZ}_4\rangle = \frac{1}{\sqrt{2}} (|0000\rangle + |1111\rangle)$.

So far we have only considered a linear chain of qubits. For higher-dimensional lattices ($d \geq 2$), every lattice site is now specified by a vector of d integers a . Each site a has $2d$ neighbors. If neighboring sites are occupied by qubits, those qubits interact with the qubit in a .

Let the set A specify all the lattice sites occupied by qubits. Two sites a and a' are connected (topologically) if there exists a sequence of neighboring occupied sites, that is,

$$\{a_j\}_{j=1}^N, \quad \text{such that } a_1 = a, \quad a_N = a'. \quad (13)$$

In this case, a cluster $C \subset A$ is a set of connected lattice sites such that the corresponding state of the cluster qubits is given by

$$|\phi\rangle_C = \bigotimes_{c \in C} \left(|0\rangle_c \bigotimes_{x \in \Gamma} Z^{(c+x)} + |1\rangle_c \right) \quad (14)$$

where Γ refers to a set of steps $\{x\}$ needed to move from site a to any adjacent site $a' = a + x$ (that

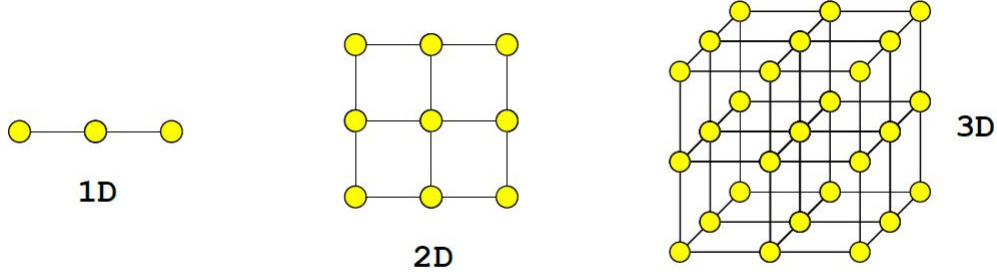


Figure 1: Examples of cluster states: linear, square (or rectangular), and cubic. The yellow dots represent qubits while the lines represent entanglement between nearest neighbors.

is, the set

$$\eta_a = \{a + x \mid x \in \Gamma\} \quad (15)$$

is the set of neighboring sites of a) and $Z_{c+x} = \mathbf{1}$ when $c+x \notin C$. Some examples of clusters of different lattice dimensions is shown in fig. (1).

Two important entanglement properties [2] characterizing cluster states are:

- (i) Maximal connectedness: Any two qubits of C_N can be projected into a pure Bell state by local measurements on all the other qubits.
- (ii) Persistency: $P_{\text{ent}}(|\psi\rangle)$ denotes the minimum number of local measurement of qubits necessary to disentangle the state $|\psi\rangle$. It turns out that this is equivalent to the Schmidt rank, the fewest number of terms in the generalized Schmidt decomposition [3]. For cluster states,

$$P_{\text{ent}}(|\phi\rangle_{C_N}) = \left\lfloor \frac{N}{2} \right\rfloor. \quad (16)$$

We note that a convenient, compact way to define a cluster state is via a set of eigenvalue equations

$$K_a |\phi\rangle_C = \kappa_a |\phi\rangle_C \quad (17)$$

where

$$K_a = X_a \bigotimes_{x \in \Gamma} Z_{a+x}, \quad \kappa_a = \pm 1. \quad (18)$$

It turns out that in the stabilizer formalism [4, 5], the operators K_a are stabilizer generators and cluster states are their corresponding eigenstates.

3 Universality of cluster-state quantum computing

3.1 Simulating quantum circuits

One can think of using the cluster state as a substrate on which quantum circuits can be imprinted on [6]. To describe this computational circuit, it is important to distinguish between the physical qubits that make up the cluster state and the logical qubits on which quantum information processing is to take place. Due to the entanglement properties of a cluster state, no individual physical qubit carries information that corresponds to an input state—rather information is contained in correlations between

qubits. However, for simplicity we first consider the case where an encoded input state is read into the cluster.

Suppose we start with an array of qubits arranged in a square lattice and whose state is given by $|\phi\rangle_C$. Then to perform a quantum computation, we do the following:

- (a) Remove the subset of qubits not needed for the calculation by measuring these qubits in the Z -basis. If the calculation uses qubits arranged in some network C' , then $|\phi\rangle_C \mapsto |S\rangle_{C \setminus C'} \otimes |\phi'\rangle_{C'}$, $|\phi'\rangle_{C'}$ is local unitarily equivalent to $|\phi\rangle_{C'}$, which is just a smaller cluster state.
- (b) To perform a specific gate, it suffices to measure the remaining qubits in a particular order and along bases that depend on the outcome of previous measurements. The last subset of qubits to be measured corresponds to the output or readout of the computation.

To show that cluster states provide a resource for universal quantum computation, we describe how any quantum circuit can be simulated efficiently on cluster states.

To propagate information through the cluster, a qubit can be teleported between any two sites by measuring the chain of qubits that connect them in the X basis. To see this, consider a linear chain of N qubits in the state

$$|\psi_{\text{in}}\rangle_1 \otimes |+\rangle_2 \otimes \dots \otimes |+\rangle_N. \quad (19)$$

which are then entangled via the pairwise CPHASE operation, which we denote with \mathcal{S} :

$$\mathcal{S} = \exp(-iH_{\text{int}}t/\hbar) = \exp \left[-i\pi \sum_a \left(\frac{1+Z_a}{2} \right) \left(\frac{1-Z_{a'}}{2} \right) \right]. \quad (20)$$

The qubit $|\psi_{\text{in}}\rangle$ can be transferred to site N by a series of X -measurements performed the qubits at sites $j = 1, 2, \dots, N-1$. If the outcomes are $s_{j,X} \in \{0, 1\}$ for $j = 1, 2, \dots, N-1$ then after the measurements, the chain will be in the state

$$|s_{1,X}\rangle_1 \otimes |s_{2,X}\rangle_2 \otimes \dots \otimes |\psi_{\text{out}}\rangle_N \quad (21)$$

where

$$|\psi_{\text{out}}\rangle = U_{\Sigma} |\psi_{\text{in}}\rangle, \quad U_{\Sigma} \in \{\mathbf{1}, X_N, Z_N, X_N Z_N\}, \quad (22)$$

in which case the input state in site 1 is recovered at site N after a suitable Pauli operation. Note that one does not need to record all the outcomes $s_{j,X}$ since there are only four possible choices for U_{Σ} —it is enough to perform the X measurements in sequence and update 2 classical bits to keep track of what U_{σ} will be. This notion of single-qubit teleportation for a cluster state generalizes to any linear chain that might be a subset of qubits within a cluster, that is, each qubit in the chain is entangled to exactly two neighboring sites (except for the endpoints).

As a simple example, let us consider a chain of 3 qubits

$$|\phi\rangle_{C_3} = CZ^{(12)} \otimes CZ^{(23)} |\psi\rangle_1 |+\rangle_2 |+\rangle_3, \quad |\psi\rangle = \alpha|0\rangle + \beta|1\rangle. \quad (23)$$

After the pairwise CPHASEs we obtain

$$\begin{aligned} |\phi\rangle_{C_3} &= \frac{\alpha}{2} (|+++ \rangle + |+-+ \rangle + |-++ \rangle + |--+ \rangle + |++- \rangle - |+- - \rangle + |-+- \rangle - |-- - \rangle) \\ &\quad + \frac{\beta}{2} (|+++ \rangle + |+-+ \rangle - |-++ \rangle - |--+ \rangle - |++- \rangle + |+- - \rangle + |-+- \rangle - |-- - \rangle). \end{aligned} \quad (24)$$

Upon measuring X_1, X_2 , then the change in the state $|\mu\rangle_3$ of qubit 3 depends on the outcomes in the

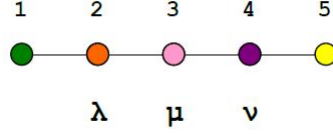


Figure 2: Simulated arbitrary single-qubit rotation in a cluster state. The angles λ, μ, ν refer to the Euler angles of the rotation implemented by $U_R(\theta)$. The sequence of measurement bases for the five qubits is described in the main text.

following way:

$$\begin{aligned} |+\rangle_{12}: |\mu\rangle_3 &= \alpha|0\rangle + \beta|1\rangle, & |+-\rangle_{12}: |\mu\rangle_3 &= \alpha|1\rangle + \beta|0\rangle, \\ |-\rangle_{12}: |\mu\rangle_3 &= \alpha|0\rangle - \beta|1\rangle, & |--\rangle_{12}: |\mu\rangle_3 &= \alpha|1\rangle - \beta|0\rangle. \end{aligned}$$

Therefore, by performing some correction $U_\Sigma \in \{\mathbf{1}, Z, X, XZ\}$ on qubit 3, we recover the state $|\psi\rangle$ at the third site. It is worth noting that in the above example, qubit 1 before measurement and qubit 3 after correcting for U_Σ is the same logical qubit—that is, no actual quantum computation has taken place yet.

Now we are ready to demonstrate how quantum gates can be simulated with cluster states. Firstly, let us show how arbitrary single-qubit rotations $U_R \in \text{SU}(2)$ is achieved with a linear cluster of five qubits, as shown in fig. (2), by considering the Euler decomposition of the rotation implemented by U_R :

$$U_R(\alpha, \beta, \gamma) = U_X(\gamma)U_Z(\beta)U_X(\alpha) \quad (25)$$

where

$$U_X(\theta) = \exp(-i\theta X/2), \quad (26)$$

and similarly for U_Z .

To see how this works, suppose site 1 carries the input qubit. Consider the state of the five qubits after the entangling operation S :

$$\mathcal{S}|\phi\rangle_{C_5} = \frac{1}{2} [|\psi_{\text{in}}\rangle_1 \otimes (|0-0-\rangle_{2345} + |0+1+\rangle_{2345}) + |\bar{\psi}_{\text{in}}\rangle_1 \otimes (|1+0-\rangle_{2345} + |1-1+\rangle_{2345})] \quad (27)$$

where $|\bar{\psi}_{\text{in}}\rangle = Z|\psi_{\text{in}}\rangle$. The input $|\psi_{\text{in}}\rangle$ can be rotated by measuring qubits 1 to 4 in the basis

$$B_j(\theta_j) = \left\{ \frac{|0\rangle + e^{i\theta_j}|1\rangle}{\sqrt{2}}, \frac{|0\rangle - e^{i\theta_j}|1\rangle}{\sqrt{2}} \right\} \quad (28)$$

where the outcomes $s_j = 0, 1$ are obtained for $j = 1, 2, 3, 4$. If $s_j = 0$, $|\psi_{\text{in}}\rangle$ is projected onto the first state of basis B_j . If $s_j = 1$, it is projected onto the second one. To perform the rotation U_R in eq. (25), we choose the bases $B_1 - B_4$ for qubits 1–4 to be

$$B_1(0), \quad B_2(-\alpha(-1)^{s_1}), \quad B_3(-\beta(-1)^{s_2}), \quad B_4(-\gamma(-1)^{s_1+s_3}). \quad (29)$$

In this case,

$$\mathcal{S}|\phi\rangle_{C_5} \mapsto |s_{1,\beta_1}\rangle_1 \otimes |s_{2,\beta_2}\rangle_2 \otimes |s_{3,\beta_3}\rangle_3 \otimes |s_{4,\beta_4}\rangle_4 \otimes |\psi_{\text{out}}\rangle_5 \quad (30)$$

where

$$|\psi_{\text{out}}\rangle = U_\Sigma U_R |\psi_{\text{in}}\rangle. \quad (31)$$

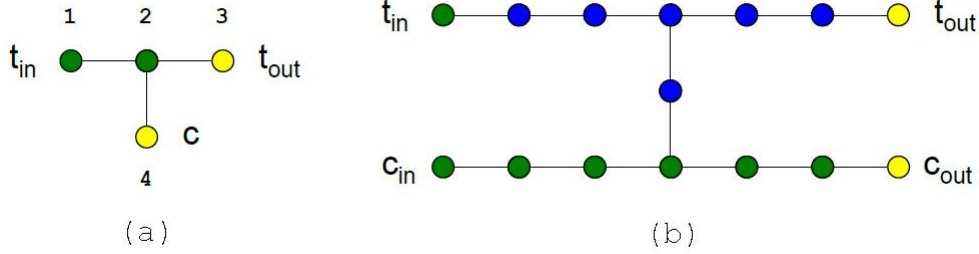


Figure 3: Simulated CNOT gate in a cluster state. (a) Minimal implementation of the CNOT gate using 4 qubits and (b) Standard CNOT gate where both the logical control qubit and the logical target qubit are teleported to other sites.

If we measure the basis in eq. (29) then

$$U_{\Sigma} = X^{s_2+s_4} Z^{s_1+s_3}, \quad U_R = U_R [(-1)^{s_1+1}\alpha, (-1)^{s_2}\beta, (-1)^{s_1+s_3}\gamma] \quad (32)$$

where U_Z encodes the Pauli errors to be corrected at the end of the computation. Observe that the Hadamard and $\pi/2$ -phase gates can be realized as special cases of U_R for suitable choice of Euler angles.

To get a universal set of gates for a quantum circuit, we will need at least one entangling two-qubit gate. In this case, we choose the CNOT gate. To perform a CNOT operation on two qubits, we may use the minimal implementation involving four qubits, as shown in fig. (3a). It is a cluster composed of three qubits in a chain with the control qubit attached as a fourth qubit, with state given by

$$|\phi_{CNOT}\rangle_{C_4} = S|i_{1,Z}\rangle_1 \otimes |i_{4,Z}\rangle_4 \otimes |+\rangle_2 \otimes |+\rangle_3. \quad (33)$$

We then measure qubits 1 and 2 in the X -basis, which projects them onto $|s_{1,X}\rangle_1 \otimes |s_{2,X}\rangle_2$, for outcomes $s_{j,X}, j = 1, 2$, that is

$$|\phi_{CNOT}\rangle_{C_4} \mapsto |s_{1,X}\rangle_1 \otimes |s_{2,X}\rangle_2 \otimes U_{\Sigma}^{(34)} (|i_{4,Z}\rangle_4 \otimes |i_1 \oplus i_4\rangle_3) \quad (34)$$

where

$$U_{\Sigma}^{(34)} = Z_3^{s_1+1} X_3^{s_2} Z_4^{s_1} \quad (35)$$

Thus, the input $|\psi_{14}\rangle$ has the qubit 1 teleported to qubit 3, where it is acted upon by a CNOT followed by Pauli rotations in $U_{\Sigma}^{(34)}$, which depend on the outcomes s_1, s_2 .

In practice, it will be more convenient to have a CNOT gate such that the control qubit is also transferred to some other site, similar to how the target qubit is moved in the minimal implementation. In this case, the preferred CNOT gate is the one with 15 qubits and involves only X and Y measurements, as shown in fig. (3b).

The set $\{CNOT, U_R(\alpha, \beta, \gamma)\}$ form a universal set of quantum gates in the network model. To simulate a multi-gated quantum circuit in a cluster state, one simply combines simulated gates such that the qubits carrying the output register of the preceding gate becomes the input register of the succeeding gate. An example of such gate concatenation is shown in fig. (4). Since these gates can be simulated and combined together using cluster states, the cluster state is indeed a universal resource for quantum computation.

For a cluster-state quantum computer designed to simulate a quantum circuit, the output of every

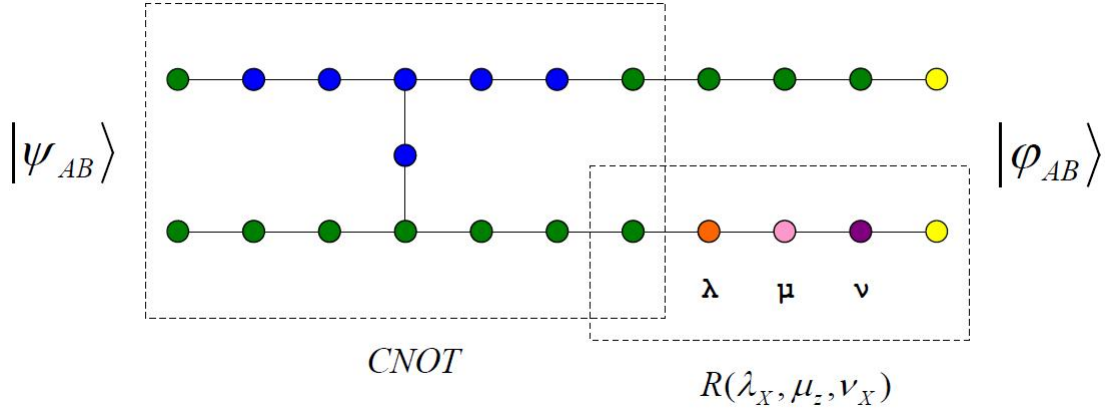


Figure 4: Concatenating simulated gates in a cluster state. For a sequence of gates in a quantum circuit, we simply concatenate gates such that the output qubit of the first gate is the input qubit of the next one, and so on.

gate becomes the input qubits for the subsequent gate in the series of gates. Note that gates in parallel in the network model can be performed in parallel, too, with cluster states.

Given a quantum circuit implemented by a network \mathcal{N} of cluster state qubits then if we suppose that \mathcal{N}_1 is the subset of cluster qubits that form gate 1 and \mathcal{N}_2 is the subset of cluster qubits that form gate 2 of circuit $\mathcal{N} = \mathcal{N}_1 \cup \mathcal{N}_2$ with two gates in series then there is an overlap $\mathcal{O} = \mathcal{N}_1 \cap \mathcal{N}_2 \neq \emptyset$ such that

$$\mathcal{O} = \text{output qubits of gate 1} = \text{input qubits of gate 2.} \quad (36)$$

There are two strategies for simulating quantum networks with cluster states:

- (a) Approach 1: Write input into select qubits and entangle \mathcal{N} . Measure subset of qubits $\mathcal{N} \setminus \mathcal{R}$. Measure readout \mathcal{R} .
- (b) Approach 2: Write input into select qubits. Entangle \mathcal{N}_1 , Measure qubits $\mathcal{N}_1 \setminus \mathcal{O}$, with output registered in \mathcal{O} . Use \mathcal{O} as input for \mathcal{N}_2 . Entangle \mathcal{N}_2 . Measure qubits $\mathcal{N}_2 \setminus \mathcal{R}$. Measure readout \mathcal{R} .

Approaches 1 and 2 are equivalent since the measurements of $\mathcal{N}_1 \setminus \mathcal{O}$ commute with the entangling operation on \mathcal{N}_2 because they act on disjoint subsets of the cluster qubits. Note that the readout qubits \mathcal{R} are typically measured in the Z -basis.

We end this section with a few remarks:

- (i) Quantum circuits can be implemented on irregularly shaped clusters with various entanglement patterns—one can generalize to different types of graph states. The universality of any irregularly-shaped cluster state is related to percolation properties of the lattice (connectedness of sites) and depends on some critical value for the site occupancy probability.
- (ii) Note that writing the input as described above is introduced only for pedagogical reasons. For any set of N entangled qubits in a cluster state, one can always find a suitable set of measurements on $N - 1$ qubits such that the remaining qubit is prepared in any desired quantum state, which can then be subsequently treated as input of a circuit. Thus, a cluster state is a genuine resource for quantum computation.
- (iii) It is always possible to split the computation into segments that require only a small number of qubits, in which case the cluster is repeatedly re-entangled after every measurement segment, except for the qubits that hold the intermediate output information.

3.2 Random measurement outcomes

Here we will illustrate that the cluster state computer works with unit efficiency despite the random nature of measurement outcomes. We will see that the byproduct operator U_Σ acting after the final unitary gate doesn't jeopardize the scheme. Its only effect is to change how the readout must be interpreted.

The byproduct operator U_Σ is such that it acts on n logical output qubits with a product of Pauli operators

$$U_\Sigma^{(n)} = \prod_{i=1}^n X_i^{x_i} Z_i^{z_i}. \quad (37)$$

Suppose that the output qubits in the cluster, just before doing readout measurements, are in the state

$$|\Phi\rangle = U_\Sigma |\psi_{\text{out}}\rangle. \quad (38)$$

Typically, these qubits are measured in the Z -basis to obtain the classical readout, yielding a set of outcomes $\{s_i\}$.

However, what we really want for the output of the algorithm are the outcomes $\{s'_i\}$ obtained if we first correct for the accumulated Pauli errors in the byproduct operator. Thus, we have two situations

$$|\psi_{\text{out}}\rangle \mapsto \{s'_i\}, \text{ and } U_\Sigma |\psi_{\text{out}}\rangle \mapsto \{s_i\}. \quad (39)$$

In terms of the outcomes s_i , the readout qubits are projected onto the state $|M\rangle$ given by

$$\begin{aligned} |M\rangle &= \prod_{i=1}^n \left[\frac{1 + (-1)^{s_i} Z_i}{2} \right] U_\Sigma |\psi_{\text{out}}\rangle \\ &= U_\Sigma \left(U_\Sigma^\dagger \prod_{i=1}^n \left[\frac{1 + (-1)^{s_i} Z_i}{2} \right] U_\Sigma \right) |\psi_{\text{out}}\rangle \\ &= U_\Sigma \left(\prod_{i=1}^n \left[\frac{1 + (-1)^{s'_i} Z_i}{2} \right] \right) |\psi_{\text{out}}\rangle, \end{aligned} \quad (40)$$

where $s'_i = s_i \oplus x_i$ are the desired results of the computation and the values x_i are determined by the byproduct operator U_Σ .

Thus, the performance of quantum circuit is uninhibited by random measurement outcomes since outcomes before and after correcting for Pauli errors just correspond to different rotations in U_Σ , which can always be tracked and corrected at the last step. Next, we describe how the byproduct operations can be propagated to the end of any quantum computation.

3.3 Sequence of simulated quantum gates

For a sequence of simulated quantum gates, we can describe the state of the cluster as

$$|\psi_{\text{out}}\rangle = \left(\prod_{i=1}^{|\mathcal{N}|} U_{\Sigma, g_i} U_{g_i} \right) |\psi_{\text{in}}\rangle \quad (41)$$

where the gates g_i are listed from right to left according to their temporal order in a circuit. In Ref. [6], this is actually Theorem 1, and its proof can be found there. Eq. (41) is actually an important result concerning the relationship between the network model and the cluster-state model because it relates unitary transformations in the network model that turn input qubits into an output register to

quantum correlations exhibited by cluster states used to simulate quantum gates.

Randomness of measurement outcomes can be propagated forward through subsequent gates such that they always act on the subset of cluster qubits that represent the output register of the corresponding network model. The propagation rules are

$$\begin{aligned} CNOT_{c,t}X_t &= X_tCNOT_{c,t}, & CNOT_{c,t}X_c &= X_cX_tCNOT_{c,t}, \\ CNOT_{c,t}Z_c &= Z_cCNOT_{c,t}, & CNOT_{c,t}Z_t &= Z_cZ_tCNOT_{c,t} \end{aligned} \quad (42)$$

for the CNOT gate with control qubit c and target qubit t , and

$$U_R(\alpha, \beta, \gamma)X = XU_R(\alpha, -\beta, \gamma), \quad U_R(\alpha, \beta, \gamma)Z = ZU_R(-\alpha, \beta, -\gamma) \quad (43)$$

for arbitrary single qubit rotations, which has special cases

$$HX = ZH, \quad HZ = XH \quad (44)$$

for the Hadamard gate and

$$U_Z(\pi/2)X = YU_Z(\pi/2), \quad U_Z(\pi/2)Z = ZU_Z(\pi/2) \quad (45)$$

for the $\pi/2$ -phase gate.

Observe that Pauli operators get mapped to Pauli operators under the propagation of the byproduct operator so U_Σ is indeed still composed exclusively of Pauli operators. However, we notice that for CNOT, Hadamard and the $\pi/2$ -phase gate, U_Σ changes without changing the gate, unlike in the case of other arbitrary rotations U_R .

In fact, for all gates $U_g \in \mathcal{C}$ that belong to the Clifford group \mathcal{C}

$$U_gU_\Sigma = (U_gU_\Sigma U_g^{-1})U_g = U_\Sigma U_g \quad (46)$$

since the Clifford group is the normalizer of the Pauli group under conjugation. Because Clifford gates are unaffected by propagating U_Σ , it implies that all Clifford gates $U_g \in \mathcal{C}$ can be measured simultaneously in the first measurement round. This fact about quantum circuits in the Clifford group was not previously known in the network model.

We remark that according to the Gottesman-Knill theorem [4], if the quantum circuit is such that it involves only Hadamard gates, CNOT gates, and Pauli gates, these Clifford circuits (stabilizer circuits) can be simulated efficiently classically. However, our point here is that the entire Clifford part of any quantum circuit can in fact be performed in a single time step. In terms of temporal complexity of a cluster state algorithm, it means that Clifford gates do not contribute (since they merely add a logical depth of 1).

3.4 Efficiency of simulating quantum gates

Although we have seen how a cluster state is used to simulate a universal set of gates, we are still left with the question of whether it does so in an efficient way. To determine this, we compare the cluster-state resources needed in simulating a quantum network and show that there is at most a polynomial overhead. To run a specific algorithm, we need a cluster of a certain size. Hence, the spatial resources S needed for cluster state computing is just $|C|$, the number of qubits in the cluster C .

The calculation is driven by single-qubit measurements exclusively. Thus, these measurements form

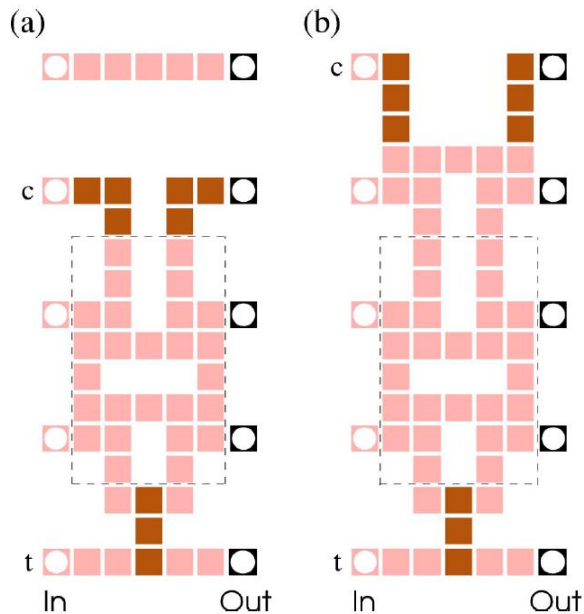


Figure 5: General CNOT for non-neighboring qubits. Squares in light brown denote cluster qubits measured in the X -basis, in dark brown for the Y -basis. Pattern (a) is for the case of qubits separated by an odd number of logical qubits. Pattern (b) is for the even numbered separation. The pattern can be adapted to any scenario by repeating the section enclosed in dashed lines. Note that the width of the pattern remains the same no matter how far apart the logical qubits are.

the operational resources O , given by their total number. It is certainly the case that

$$O \leq S \tag{47}$$

since each cluster qubit is measured at most once.

The temporal resources T have to do with the minimum number of measurements that can be performed in parallel, which we will compare with the number of layers of gates or logical depth in the network model.

We have seen the universality of cluster state computing in terms of its ability to simulate CNOT and single-qubit rotations, which form a universal set of quantum gates. Now we look for the upper bounds in resources used for the cluster state simulation and compare it with their network model counterparts.

Concerning temporal resources T , for general qubit rotations—assuming this can be done in one step in a quantum gate circuit—we will need at most three time step for every such single-qubit unitary due to the Euler decomposition angles. Thus,

$$T \leq 3T_n \tag{48}$$

Concerning spatial resources S , we first have to note that for the CNOT, there might be an issue with regard to logical qubits that are far apart. What we have considered previously is only the case where the control and target qubits are effectively nearest neighbor. However, we might want to perform a CNOT between two cluster qubits that are much farther apart and there is a question of how the necessary swapping or teleportation of qubits scales with the distance of the qubits.

However, it turns out that it is possible to use a different measurement pattern indicated in fig. (5), what we call a general CNOT gate. The advantage of this general CNOT is that there is a fixed

cluster size added in between the pair of qubits on which the CNOT is performed, so that the spatial complexity scale only linearly with the distance of the two qubits. Also with this general CNOT, the logical qubits are at most 4 cluster qubits apart and the width from input to output can be made to be at most 6.

With that in mind, we can calculate the upper bound on $S = hw$ to be

$$S \leq 24S_n^2T_n \tag{49}$$

since the height $h \leq 4S_n$ is bounded by the distance of logical qubits for the possible instance of CNOT gates and the width $w \leq 6S_nT_n$ is bounded by the width of the general CNOT and the fact that the corresponding simulated quantum network would have at most S_nT_n gates.

The main purpose of this section was to show that gate simulation by cluster states is at most polynomial in resources compared to the associated quantum circuit. It must be mentioned that the classical processing for determining the adaptive measurement bases just adds a marginal overhead to the algorithm (it adds complexity $O(\log n)$, where n is the number of logical qubits in the computation).

4 Computational model for the cluster-state quantum computer

4.1 Non-network character of cluster state computing

In the quantum network model, one prepares the input state in a quantum register and processes the quantum information through a sequence of quantum gates that apply suitable unitary transformations to the state, yielding an output state that is measured to obtain a classical readout.

Although we have demonstrated how quantum circuits may be simulated using cluster states, the notions of quantum input and output have no genuine meaning if one considers an algorithm for which the input state is known. For instance, Shor’s algorithm always starts with the input in the state

$$|\Psi\rangle = \bigotimes_{j=1}^N \frac{|0\rangle_j + |1\rangle_j}{\sqrt{2}} = |+\rangle^{\otimes N} \tag{50}$$

In fact, without loss of generality, we may assume that the input state $|\Psi\rangle$ is read onto a subset of some cluster C . Reading in the input $|\Psi\rangle$ means preparing

$$\mathcal{S} \left(|+\rangle^{\otimes M} \otimes |+\rangle^{\otimes (N-M)} \right) = |\phi\rangle_C, \tag{51}$$

that is, preparing a cluster state in the usual way. Thus, a cluster state $|\phi\rangle_C$ is a universal resource that does not depend on any input information. It is in this sense that cluster states have no quantum input.

The cluster state also has no true notion of a quantum output because unlike a quantum network where the output register has a distinguished role before the readout measurements are performed, the cluster qubits that carry the readout information are no different from other cluster qubits in that they are to be measured in some particular order or basis. In fact, it is not uncommon to have the the readout qubits to be among the first qubits to be measured—since typically, these readout qubits are measured in the Z -basis—making it somewhat inappropriate to treat them as output qubits in the sense of the network model.

Measurement outcomes from all cluster qubits contribute to the computation. Suppose we consider

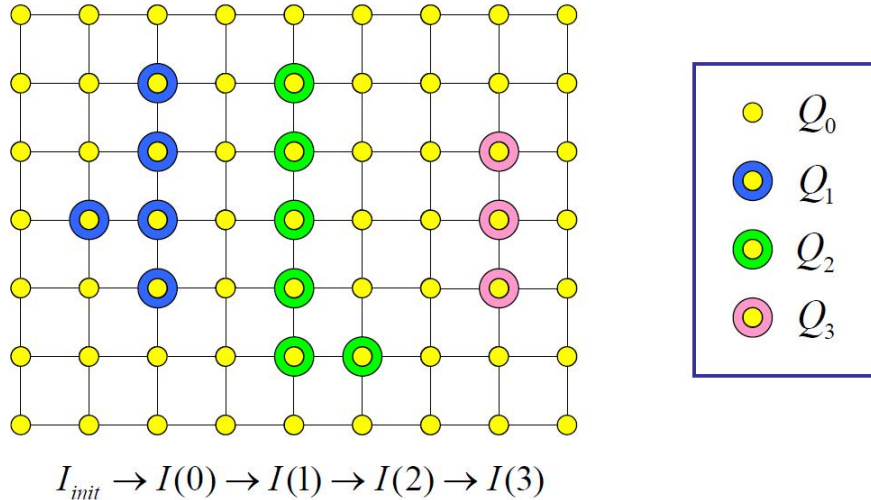


Figure 6: Computational model for cluster state computing. The cluster is divided into disjoint subsets labeled according to temporal order, where the bases of adaptive measurements are determined using an information flow vector $\vec{I}(t)$ that is updated at each time step.

a cluster C that is divided into disjoint subsets of qubits $O \cup I \cup M = C$, then

- (a) O simulates the output register from which the readout will be obtained;
- (b) I simulates the fiducial input state and contributes to the calculation via the accumulated byproduct operator U_Σ , which carries the information for correcting Pauli errors;
- (c) M simulates the unitary gate operations via the initial quantum correlations present in the cluster state and adaptive single-qubit measurements.

4.2 A cluster-state computational model

Single-qubit measurements form the basic building blocks of cluster-state computing, not quantum gates [7]. The most efficient temporal order does not follow from temporal order of simulating quantum circuits but instead follows a set of rules that determine efficient conditional processing of the adaptive measurements. Central to the conditional processing paradigm (and thus, the computational model) is an object called the information flow vector $\vec{I}(t)$, which tracks the classical information needed for carrying out subsequent measurements based on the outcome of previous ones.

Cluster state computing works by measuring correlations encoded in the massively entangled initial state of the cluster and processing these via a sequence of adaptive measurements tailored to do a particular algorithm. Because these quantum correlations are available at the onset of the computation, there is no quantum information processing during the cluster state computation itself.

From the conceptual point of view—and also useful to the practical realizability of the scheme—it is important to realize that the correlations in the cluster state can be measured one qubit at a time. This corresponds to classical conditional processing once the temporal order of single-qubit measurements is established.

From this we may view the cluster state computation in the following way: The cluster C is divided into temporally-ordered disjoint subset of qubits $Q_t \subset C, 0 \leq t \leq \tau$, that is,

$$\bigcup_{t=0}^{\tau} Q_t = C, \quad Q_s \cap Q_t = \emptyset \quad \forall s \neq t. \quad (52)$$

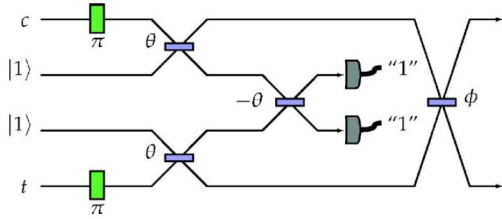


Figure 7: Knill CZ gate. Beamsplitters are at angles $\theta = 54.74^\circ$ and $\phi = 17.63^\circ$ yielding transition amplitudes $\cos \theta$ and $\cos \phi$, respectively.

Cluster qubits within each subset Q_t can be measured simultaneously. The set Q_0 corresponds to those qubits whose measurement bases are fixed, i.e., they do not depend on the outcome of other measurements. These measurements will be those corresponding to Pauli bases, which is also called the Clifford part of the circuit.

For $t > 0$, Q_t involves only measurement operators of the form

$$\cos \varphi X \pm \sin \varphi Y, \quad 0 < |\varphi| < \frac{\pi}{2}. \quad (53)$$

where the \pm depend on some of the previous measurement outcomes.

The sequence is such that Q_1 depends on outcomes of Q_0 , Q_2 depends on outcomes of Q_0 and Q_1 , and so on. The result of the computation is calculated from outcomes of all measurement rounds (using information encoded in the readout qubits and the accumulated byproduct operator U_Σ).

Thus, the computational model of cluster state computing [7] can be characterized by the following:

- (i) temporal order of single-qubit measurements divides the cluster into disjoint subsets;
- (ii) spatial pattern of measurements corresponds to particular manipulations of correlations among cluster qubits—simulating the effect of quantum gates;
- (iii) the information flow vector $\vec{I}(t)$ carries the classical information needed to steer the computation forward, since it specifies the adaptive bases required at each time step.

A schematic of the computational model is illustrated in fig. (6).

5 Optical implementation of cluster states

5.1 Cluster states and the Knill-Laflamme-Milburn (KLM) proposal

An attractive approach to practical implementations of quantum computing would be the use of linear optical devices because photons have long decoherence times and are relatively easy to manipulate in the lab. The scheme introduced by Knill, Laflamme and Milburn in 2001, called the KLM proposal [9] demonstrated that a fully optical quantum computer using just beamsplitters, phase shifters, single photon sources and photodetectors is possible, in principle. The biggest challenge with photons was performing a two-qubit entangling quantum gate, which was shown to be achievable near-deterministically if one combines the probabilistic nonlinear gates of KLM with teleportation. In this case, one obtains a near-deterministic CZ gate, which we will denote as $CZ_{n^2/(n+1)^2}$, to indicate that the gate has success probability $n^2/(n+1)^2$. One can then increase the probability of success by using techniques of quantum error correction.

The problem with combining all of these elements together is that it makes the implementation very complicated very quickly, requiring thousands of optical devices for a marginally larger success rate. Nielsen then improved on the KLM analysis by combining the non-deterministic CZ gates with the

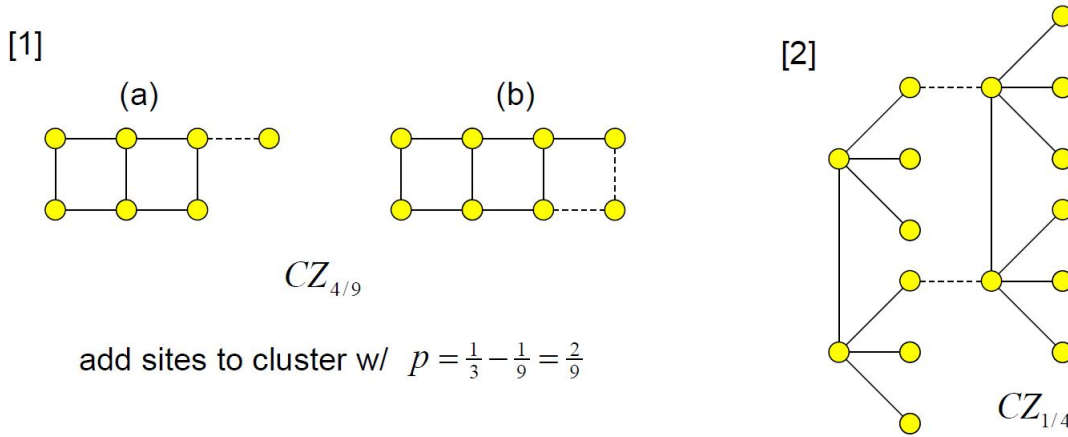


Figure 8: Adding sites to an optical cluster state. [1] Two ways to add a qubit to the cluster with $CZ_{4/9}$ gates: (a) with a single bond and (b) with a double bond. [2] One can also form smaller clusters with dangling nodes that are attached together using $CZ_{1/4}$ gates.

cluster state model, greatly reducing the overhead for additional success. We briefly describe Nielsen’s scheme here.

Fig. (7) shows the Knill CZ gate, a simplification of the original CZ gate in the KLM proposal. It takes two logical qubits as input and with probability $2/27$ applies a phase gate, or else fails, destroying the two qubits. It uses 2 phase shifters, 4 beamsplitters and 2 photodetectors for measuring the ancillas—these must distinguish 1 photon signal from that of 0 or 2 photons.

The Knill CZ gate can be improved by combining it with gate teleportation, which increases the success rate to $n^2/(n+1)^2$. When the gate fails, it performs a Z -measurement on the control qubit of the operation.

The basic $CZ_{n^2/(n+1)^2}$ gate involves two teleportation steps in parallel, each with independent success probabilities $n/(n+1)$. It is possible to do the teleportations in sequence rather than in parallel so that one can simply abort the gate if the first teleportation process fails. It is the sequential method that is advantageous to use in the cluster state model. The idea is to create a cluster state by non-deterministically adding extra qubits using $CZ_{4/9}$ or $CZ_{1/4}$ gates.

The cluster is built up from two types of operations that add a site or qubit, either with a single or a double bond, as shown in fig. (8.1). The procedure to add a single-bonded site is to use the $CZ_{4/9}$ gate, which succeeds in adding a cluster site with probability $2/3$. When it fails, it measures a qubit in the Z -basis and effectively removes it from the cluster. Thus, the average number of sites it adds to the cluster is given by $2/3 - 1/3 = 1/3$. Similarly, the procedure to add a double bonded-site is to use two $CZ_{4/9}$ gates, which can be done in sequence so that one aborts the procedure when the first one fails. In this case the average number of sites added is $(2/3)(2/3) - 1/3 - (1/3)(2/3) = -1/9$. If the single and double bonded procedures are used equally, then the expected number of sites added to the cluster is at least $1/3 - 1/9 = 2/9$. Thus, a cluster of size N can be grown using approximately $9N$ attempts to add a single site.

One can also grow the cluster state by first preparing smaller clusters or micro-clusters with many dangling nodes, as shown in fig. (8.2). These micro-clusters are then glued together at some of the nodes using parallel $CZ_{1/4}$ gates. By increasing the number of dangling nodes, we can increase the probability of successful gluing.

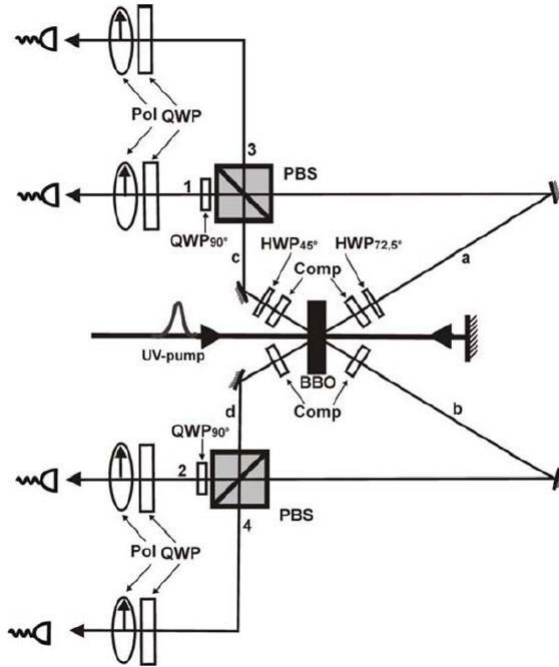


Figure 9: *Experimental setup for creating cluster states. Two entangled pairs of photons are created by two passes of a frequency doubled laser pulse through a nonlinear crystal. Using half-wave plates and compensation crystals, the entangled pairs can be prepared in any Bell state. They are then combined using polarizing beamsplitters into a four-qubit cluster state in the polarization.*

5.2 Practical optical cluster state

The earliest practical realization of an optical cluster state was achieved in an experiment by Walther et. al [10], where they created a four-qubit cluster state encoded in the polarizations of four photons. We describe the methods here briefly.

The experimental setup is shown in figure (9). Entangled photons are created using parametric down-conversion. Using a frequency doubled laser pulse at 395 nm that is made to pass twice through a nonlinear crystal (BBO), two highly entangled photon pairs are produced in modes a-d.

After correcting for birefringence due to the BBO crystal, half-wave plates and compensation crystals are used to produce any Bell state for each entangled pair. The photon pairs are finally combined in a coherent way using a polarizing beamsplitter, where the four photons end up in the cluster state

$$|\phi_{C_4}\rangle = \frac{1}{2} (|HHHH\rangle + |HHVV\rangle + |VVHH\rangle - |VVVV\rangle), \quad (54)$$

where H, V refer to horizontal and vertical polarizations, respectively. This cluster state is local unitarily equivalent to a linear cluster under the unitary

$$U_{\text{linear}} = H_1 \otimes \mathbf{1}_2 \otimes \mathbf{1}_3 \otimes H_4 \quad (55)$$

on the polarization qubits and to a box cluster state of four qubits under the unitary

$$U_{\text{box}} = \text{SWAP}_{2,3} (H_1 \otimes H_2 \otimes H_3 \otimes H_4). \quad (56)$$

In the experiment, the cluster state was verified by performing quantum state tomography, which extracts the density operator for the system from a discrete set of measurements—in this case it was

reconstructed using linear combinations of 256 linearly independent four-photon polarization projections.

6 Concluding remarks

In a seminal paper in 2001, Briegel and Raussendorf proposed an alternative model for quantum computing based on single-qubit measurements of a highly entangled multi-qubit system called a cluster state. In this project, we showed how cluster state computing can be regarded as a simulator of quantum networks by showing how it can efficiently simulate $\{CNOT, U_R(\alpha, \beta, \gamma)\}$, which forms a universal set of quantum gates. This perspective of cluster states clarifies the connection between the conventional network model of quantum computation with the cluster state computational model, which is characterized by the absence of input and output registers, a temporal ordering of single-qubit measurements, and an information flow vector that tracks the adaptive bases at each time step. Thus, it provides us with a different paradigm for quantum computing, which instead of entangling two-qubit gates has entanglement built into the resource state at the beginning and where the quantum computation proceeds through adaptive measurements. Finally, we saw how the original KLM proposal for optical quantum computing can be adopted to perform quantum computation using cluster states, and how a four-qubit cluster state in the photon polarizations was first realized experimentally.

References

- [1] R. Raussendorf, H. J. Briegel, “A one-way quantum computer,” *Physical Review Letters* **86** (2001) 5188-91.
- [2] H.J. Briegel, R. Raussendorf, “Persistent entanglement in arrays of interacting particles,” *Physical Review Letters* **86** (2001) 910-13. Also available as arXiv:quant-ph/0004051 (2000).
- [3] W. Dür, G. Vidal, J. I. Cirac, “Three qubits can be entangled in two inequivalent ways,” *Phys. Rev. A* **62** (2000) 062314. Also available as arXiv:quant-ph/0005115 (2000).
- [4] M. Nielsen, I. Chuang, *Quantum Information and Quantum Computation* (Cambridge University Press, Cambridge, 2000) 453-472.
- [5] D. Gottesman, “Stabilizer Codes and Quantum Error Correction,” PhD Thesis, California Institute of Technology (1997). Available online as arXiv:quant-ph/9705052 (1997).
- [6] R. Raussendorf, D. E. Browne, H. J. Briegel, “Measurement-based quantum computation with cluster states,” *Physical Review A* **68** (2003) 022312. Also available as arXiv:quant-ph/0301052 (2003).
- [7] R. Raussendorf, H. J. Briegel, “Computational Model for the One-Way Quantum Computer: Concepts and Summary,” arXiv:quant-ph/0207183 (2002).
- [8] M. A. Nielsen, “Cluster-state quantum computation,” *Reports on Mathematical Physics* **57** (2006) 147-161. Also available as arXiv:quant-ph/0504097 (2005).
- [9] E. Knill, R. Laflamme, G. J. Milburn, “A scheme for efficient quantum computation with linear optics,” *Nature* **409** (2001) 46-52.
- [10] P. Walther, K. J. Resch, T. Rudolph, E. Schenck, H. Weinfurter, V. Vedral, M. Aspelmeyer, A. Zeilinger “Experimental one-way quantum computing,” *Nature* **434** (2005) 169-76. Also available as arXiv:0503126 (2005).